Vehicle System Dynamics

ISSN: 0042-3114 (Print) 1744-5159 (Online) Journal homepage: https://www.tandfonline.com/loi/nvsd20

A method for estimation of vehicle inertial parameters

Matthew Rozyn & Nong Zhang

To cite this article: Matthew Rozyn & Nong Zhang (2010) A method for estimation of vehicle inertial parameters, Vehicle System Dynamics, 48:5, 547-565, DOI: 10.1080/00423110902939863

To link to this article: https://doi.org/10.1080/00423110902939863

Published online: 10 Mar 2010.

Submit your article to this journal

Article views: 1820

View related articles

Citing articles: 10 View citing articles

Full Terms & Conditions of access and use can be found at
https://www.tandfonline.com/action/journalInformation?journalCode=nvsd20

Vehicle System Dynamics
Vol. 48, No. 5, May 2010, 547–565

Taylor & Francis
Taylor & Francis Group

A method for estimation of vehicle inertial parameters

Matthew Rozyn* and Nong Zhang

Mechatronics and Intelligent Systems, Faculty of Engineering, University of Technology, Sydney, P.O. Box 123, Broadway, NSW 2007, Australia

(*Received 11 August 2008; final version received 31 March 2009; first published 10 March 2010*)

In this paper, a new method is presented for estimating the current sprung mass inertial parameters of a vehicle, such as the mass, pitch and roll mass moments of inertia, and lateral and longitudinal centre of gravity locations. The method measures the sprung mass response when the vehicle is driven over an unknown and unmeasured random road profile. From these measurements, the equivalent free-decay responses are extracted and modal analysis techniques used to estimate the sprung mass natural frequencies, damping ratios and mode shapes. This information is combined with a simplified vehicle estimation model, least squares analysis and known equivalent stiffness parameters to estimate the vehicles' inertial parameters. The results obtained from several simulation examples show that estimates of the inertial parameters generally have small relative errors.

Keywords: estimation of inertial parameters; vehicle dynamic model; vehicle system parameter identification; experimental modal analysis; least squares estimation

1. Introduction

During the lifetime of any vehicle it will be loaded in multiple configurations that will directly alter the inertial properties of mass, mass moments of inertia and centre of gravity locations. These changes in load and load distribution can be large when compared with the weight of the empty vehicle; for example, in small and light passenger vehicles, four occupants can represent upwards of a 20% change in vehicle weight, with pickups, sports utility vehicles (SUVs) as well as commercial and industrial vehicles having much larger percentage changes. These altered inertial parameters will have a direct impact on the handling [1–5], ride [5–8], braking and traction [9–11] performance of the vehicles noted above. These effects are well documented in the literature and the above references are by no means exhaustive.

As a consequence of these changes to the vehicle inertial parameters, the active control systems are likely to be affected due to discrepancies between the physical and modelled dynamics of the vehicle; for example active steering control [2,12,13], brake systems [9,12–15], ride control [16,17], driveline and traction control [14,17,18], automatic transmission control [11,15,19] and cruise control systems [20–24] are all affected by these changes. Modern

*Corresponding author. Email: mrozyn@gmail.com

ISSN 0042-3114 print/ISSN 1744-5159 online
© 2010 Taylor & Francis
DOI: 10.1080/00423110902939863
http://www.informaworld.com

vehicles employ many active control systems to improve vehicle safety, comfort, performance and efficiency; typical examples include electronic stability control (ESP), traction control (TCS), and automatic transmission systems. The operation of these control systems are predominantly based on dynamic models of the vehicle that often require vehicle inertial parameters such as mass, centre of gravity and mass moments of inertia to be known. In the absence of real-time estimates, these active control system often used fixed values for the inertial parameters that lie somewhere between the maximum and minimum expected values. The major reason for this approach is the difficulty, complexity and cost associated with measuring the inertial parameters in real time during the life of the vehicle.

The authors believe that vehicle controllers that can adapt the control strategy based on the current inertial parameters and dynamics of the vehicle will be the next logical progression of modern vehicle controllers. For example, knowledge of a loading condition that increases the chances of a vehicle oversteering may allow for pre-emptive correction of the yaw rate before, not after, the at-limit condition has been reached. This will require knowledge of the mass, centre of gravity and mass moments of inertia.

Several methods exist that can measure some of the inertial parameters of mass, centre of gravity and mass moments of inertia. *In situ* methods include pendulum test rigs [24,25] while on road methodologies can generally be classified into four categories based on the estimation models used: longitudinal, yaw, roll and bounce. The most prevalent methods in the literature are based around longitudinal dynamic equations of motion [26–34]. These types of estimators appear simple but are limited by the input forces being very hard to measure or estimate accurately, such as aerodynamic drag, road friction and changing gravity forces due to the road grade. The estimation accuracy of the mass is entirely dependent on accurate measurement of the input forces, with estimation errors ranging from 1.7% [27] to over 20% noted in the literature [28]. Longitudinal estimators can only measure the vehicle mass; estimates for the centre of gravity or mass moments of inertia are not possible using longitudinal estimators.

Yaw and roll models are also prevalent in the literature [9,33–38] but require very accurate tyre models to estimate the input forces. The accuracy of the estimator is entirely dependent on the type and accuracy of tyre model which are highly variable and change based on tyre brand, wear and inflation pressures, with errors of up to 20% reported [35].

The last major type of estimator involves the vertical bounce motion [39–41]. These methods are the least prevalent in the literature and involve measuring the input tyre forces, sprung mass acceleration and suspension deflections. These measurements dramatically increase the installation cost and complexity, and as a consequence are not widely used.

From this brief review it can be seen that the majority of estimators require the input forces to be measured or estimated. Some of these forces are variant with time (road grade, aerodynamic and friction forces) and other forces are non-linear or difficult to model accurately, for example the tyres in the lateral and longitudinal directions. If the input forces are not measured accurately, the estimation of the inertial parameters deteriorates with errors over 20% possible. To reliably measure these forces, and as a consequence estimate the inertial parameters, requires many sensors which increases cost, complexity and reduces the chances of adaptive controllers being implemented.

2. Proposed methodology

The following methodology is devised as a way to estimate the vehicle inertial parameters to an acceptable level of accuracy using the measured sprung mass system response only. This has

the double benefit of decreasing cost and reducing the estimator's reliance on measurement of the input forces. Another benefit of the proposed methodology is once the inertial parameters have been measured an estimate of the non-linear tyre forces is possible [42], further increasing the accuracy of information provided to active vehicle controllers.

The proposed method is based on modal parameter estimation using the free-decay responses of the vehicle, estimation of the system characteristic matrix using state space methods, least squares analysis, combined with a simplified vehicle model. Knowledge of the vehicle's equivalent linear spring stiffness is also required. This is a valid assumption in the opinion of the authors; this information is well known by the vehicle manufacturers and can be measured, is reasonably linear for vehicles such as passenger cars, SUVs and pickups and has much less parameter variation than damping coefficients, aerodynamic drag, road friction forces or varying gravity forces due to changes in road grade.

2.1. *Measurement sensors*

The number, location and type of sensors mounted onto the vehicle's sprung chassis mass will determine the maximum degrees of freedom, what parameters can be measured and the mathematical basis for the estimation model. An overview of sensors and sensor location is presented in this section.

The first step is to choose the type of sensors, linear or angular, to be mounted onto the vehicle chassis. For simplicity and proof of concept, the examples presented in this paper uses three accelerometers mounted to the vehicle chassis, allowing for estimates of the sprung mass, pitch and roll mass moments of inertia as well as lateral and longitudinal centre of gravity locations of the vehicle. With this configuration, measurement of the yaw inertia is not strictly possible; however, it is well documented in the literature [24,25] that the yaw and pitch inertia values are within a few percentage points of each other, and therefore a measurement of the pitch inertia will yield a reasonable estimate of the current yaw mass moment of inertia. Other sensors such as gyroscopes or Linear Variable Differential Transformers (LVDTs) can also be used.

The location of the sensors is also very important. If only accelerometers are used then they should be spaced as far apart as possible to maximise the signal-to-noise ratio of the phase and amplitude information. Another important consideration for positioning the accelerometers is related to the wheelbase filtering effect. Most frequency components that excite vehicle vibrations come from the road surface, but the geometric properties of the vehicle can result in an amplification or attenuation of certain frequencies due to the front and rear axles following the same profile delayed in time. This phenomenon is known as wheelbase filtering and is dependent on the speed of the vehicle and the wheelbase. Best [43] shows that accelerometers placed near the centre of the wheelbase will display null points and false resonance peaks. Accelerometers placed further away from the centre of gravity position, for example above the wheel stations, will detect both the bounce and pitch modes and the effect of wheelbase filtering is minimised. Therefore, in the opinion of the authors, the optimum location for accelerometers to minimise wheelbase filtering effects and to maximise the signal-to-noise ratio for phase information is at the outer edges of the vehicle. For simplicity, in this paper the sensors are placed directly above the unsprung masses, but this does not preclude other locations.

2.2. *Extraction of free-decay response*

The method relies on the successful extraction of the dynamic system's free-decay response. The method for extracting the free-decay response is dependent on the type of input to which

the vehicle is subjected: deterministic (single, impulsive type input) or stochastic (a series of random and interfering inputs). For the simplistic case of a deterministic input, the free-decay response can be found by a peak detection algorithm, and assuming this point represents the start of the free-decay response. For the more complex stochastic case presented in this paper, methods such as the random decrement technique [44] or autocorrelation function can be used to extract the equivalent free-decay response of the vehicle chassis when subject to random road excitations.

The autocorrelation function will be used for the examples in this paper. The autocorrelation of random data describes the general dependence of the values of the data at one time on the values at another time [45]. Because the vehicle's free-decay response persists over all time displacements, as opposed to random data which diminishes towards zero for large time displacements, the autocorrelation function provides a useful tool for determining trends that may be masked by random data or noise.

For the case where the excitation to the system is stationary Gaussian white noise, the autocorrelation of the response is proportional to the free vibration response [46–48]. In reality, roughness surveys have concluded that road profiles are random in nature, but follow a defined spectral density profile in the frequency domain [49] and are therefore not strictly white Gaussian. Therefore, the autocorrelation functions will not be exactly equivalent to the free-decay response in a strict mathematical sense. The specific case of white Gaussian excitation rarely holds in real-world applications and a certain amount of error must be accepted when using this approach, as detailed in [50]. It is subsequently shown, by way of analysis of the final results, that this assumption does not contribute greatly to estimation errors.

2.3. *Estimating the state transition matrix*

This section details how the state transition matrix for the dynamic system is obtained using the equivalent free-decay response. Practical implementation issues, such as the number of pseudo-measurements required to be added to the state transition matrix or frequency resolution are not discussed and the interested reader is referred to the references provided in this section.

When measurements are made at fixed resolutions (which are not infinite), the calculations must be performed in the discrete Z plane. Several methods exist to calculate the state transition matrix from discrete sensor measurements including the Ibrahim time domain method [51] and the state variable method [52,53]. The state variable method is used in this paper and a brief summary of the method is provided for completeness. In a state space representation, the system can be described by the following finite difference equation in the discrete time domain

$$\bar{\Phi} = A_1 \Phi + \tilde{\Phi} \tag{1}$$

where $\tilde{\Phi}$ represents the measurement noise matrix, A_1 the state transition matrix, and the state vectors are defined as

$$\Phi = \{X(1), X(2), \ldots, X(N)\} \tag{2}$$

$$\bar{\Phi} = \{X(2), X(3), \ldots, X(N+1)\} \tag{3}$$

$$X(k) = \{Y^{\mathrm{T}}(k) Y^{\mathrm{T}}(k+1) \ldots Y^{\mathrm{T}}(k+p)\}^{\mathrm{T}} \tag{4}$$

where $X(k)$ is the discrete vector of measurements and p is the parameter chosen according to the number of degrees of freedom and the signal-to-noise ratio of the measurement. N is the number of measurement points and Y represents the sensor measurements. The state transition

matrix A_1 can then be determined by using the least squares estimation method

$$A_1(\bar{\Phi}\Phi^{\mathrm{T}})(\Phi\Phi^{\mathrm{T}})^{-1}. \tag{5}$$

Solving the eigenvalue problem of the state transition matrix A_1 gives the eigenvalues and eigenvectors on the Z plane. Standard equations, as found in [52,53], are then used to find the system's natural frequencies, damping loss factors and mode shapes. Not all the detected natural frequencies and mode shapes will be those of the vehicle. Some false frequency and mode shape estimates will be due to computational modes, while other false estimates will be due to other transient signals or measurement noise being present in the extracted free-decay response. These are generally referred to as noise modes and need to be detected and removed prior to forming the system characteristic matrix.

The first property used for detection of noise modes is the requirement for eigenvalues to appear in complex conjugate pairs if the system is underdamped. For the bounce, pitch and roll modes on vehicles, the sprung mass damping ratios will be underdamped; therefore a result having no complex conjugate can be assumed as a noise mode. The second detection property employed is the range of frequencies and damping ratios for the vehicle sprung mass is assumed known, therefore this information can be used to detect and eliminate noise modes that lie outside this region. These are not unreasonable assumptions: vehicle manufactures will have access to this information, plus it is well known that the sprung chassis mass bounce, pitch and roll frequencies lie within the 1–3 Hz range and are underdamped with damping loss factor between 0.1 and 0.5 (vehicle dependant).

2.4. *Estimating the system characteristic matrix*

Once the noise modes have been detected and removed, the eigenvalues (natural frequencies and damping ratios) and eigenvector matrices (mode shapes) can be used to formulate the system characteristic matrix A in the continuous S plane according to the following equation [52]:

$$A = \begin{bmatrix} \lambda & \lambda^* \\ \lambda\Psi & \lambda^*\Psi^* \end{bmatrix} \begin{bmatrix} \Psi & 0 \\ 0 & \Psi^* \end{bmatrix} \begin{bmatrix} \lambda & \lambda^* \\ \lambda\Psi & \lambda^*\Psi^* \end{bmatrix}^{-1} \tag{6}$$

where Ψ is the eigenvector matrix, λ is the diagonal eigenvalue matrix and * is the complex conjugate. The system characteristic matrix A relates the mass, stiffness and damping matrices through the following equation:

$$A = \begin{bmatrix} 0 & I \\ -M^{-1}K & -M^{-1}C \end{bmatrix} \tag{7}$$

where I is the identity matrix, M is the mass matrix, C is the damping matrix and K is the stiffness matrix. The size of the characteristic matrix A is $2n \times 2n$ where n is the number of degrees of freedom. From Equations (6) and (7) it can be seen that the relationships between the mass, stiffness and damping matrices can be found from the measured free-decay responses of the vehicle.

2.5. *Estimating the inertial parameters*

The final part of the methodology involves using a simplified vehicle model, knowledge of the suspension equivalent stiffness properties and an error minimisation algorithm to estimate the vehicles mass, centre of gravity and mass moments of inertia.

2.5.1. *Vehicle estimation model*

The location, number and type of generalised co-ordinates for the vehicle estimation model must match exactly the location, number and type of sensors used to measure the response of the vehicle. The rationale behind this statement is that the mode shapes and characteristic matrices are position-dependent, and therefore discrepancies between the measured and modelled generalised coordinates will lead to inaccurate mode shapes. This will cause the estimated characteristic matrix to be incorrect when calculated using Equation (6) and subsequently lead to errors in the estimated inertial parameters.

The simplified estimation model does also not include the unsprung masses, which are around $\frac{1}{10}$th the weight of the sprung mass and thus do not significantly alter the sprung mass frequencies and mode shapes. Inclusion of the unsprung masses in the estimation model would require additional measurement sensors, increasing cost and complexity for minimal gain in accuracy. Not including the unsprung masses requires the tire and suspension springs need to be combined into a spring of equivalent stiffness. The chassis, engine, passengers and cargo are all assumed to act as a single rigid body mass in the estimation model. Finally, the estimation model assumes that the measurement sensors are aligned with the principal moment of inertia axis. This implies that the products of inertia will be estimated as zero and will result in some error on the I_{xx} and I_{yy} principal moment of inertia terms. This error is dependant on the angular difference between the sensor and principal moment of inertia axis and is not the focus of this paper.

2.5.2. *Equivalent stiffness*

As noted previously, knowledge of the equivalent stiffness parameters is required for this method of estimating the inertial parameters. The equivalent stiffness values are a combination of all parallel and in-series stiffness elements such as tyres, coil springs, leaf spring, bushings and linkages. In the literature, it is common for the following equation to be used when calculating the equivalent stiffness of springs in series.

$$k_{\text{eq}} = \frac{(k_{\text{s}} k_{\text{t}})}{(k_{\text{s}} + k_{\text{t}})} \tag{8}$$

where k_{eq} is the equivalent stiffness, and for this example k_{t} is the tyre stiffness and k_{s} is the suspension stiffness. The authors have found that the use of this equation gives unacceptably large errors due to the presence of non-proportional damping and should not be used. This equation can be derived to include for the effects of damping using quarter car theory, as shown in Figure 1.

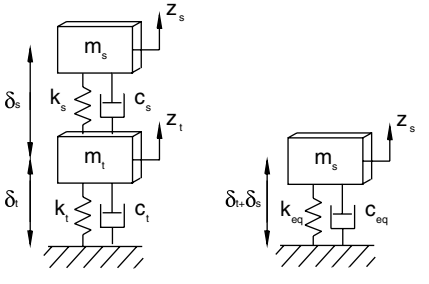

Figure 1. Free body diagrams.

Equating the 2DOF and 1DOF models yields the following equivalent stiffness equation [53]:

$$k_{\text{eq}} = \left(\frac{k_{\text{s}} k_{\text{t}}^2 + k_{\text{s}}^2 k_{\text{t}} + \omega^2 (k_{\text{s}} c_{\text{t}}^2 + k_{\text{t}} c_{\text{s}}^2)}{(k_{\text{s}} + k_{\text{t}})^2 + \omega^2 (c_{\text{s}} + c_{\text{t}})^2} \right) \tag{9}$$

where c_{t} is the tyre damping, c_{s} is the suspension damping, c_{eq} is the equivalent damping, k_{t} is the tyre stiffness, k_{s} is the suspension stiffness, k_{eq} is the equivalent stiffness, δ_{t} is the tyre deflection and δ_{s} is the suspension deflection. If damping is set to zero, Equation (9) reduces to the standard equivalent stiffness equation (8). This equation is theoretically sound, but has practical implementation issues, such as heating or degradation of the damper oil altering the damping coefficients.

An alternative is to use the damping ratio information (damping loss factor). This information can be measured using the state variable method and will yield the current damping of the vehicle, including for any changes due to heat or degradation of the dampers. This would involve deriving an equivalent stiffness equation in terms of damping ratio which is not possible for the majority of dynamic problems. For any problem with more than one degree of freedom, the roots of the characteristic equation can not be solved analytically, meaning that an equivalent stiffness equation in terms of damping loss factor cannot be found. Practically this means the equation must be derived numerically and as a consequence this equation will be vehicle-dependant. Details of the equivalent stiffness equations used in this paper can be found in Section 3.3, and more detailed information can be found in [54].

2.5.3. *Error minimisation*

The error minimisation scheme takes the measured system characteristic matrix obtained from the free-decay responses and compares it to the estimated system characteristic matrix using the simplified vehicle model. The standard least squares error minimisation formula is used as shown below.

$$S = \sum_{i-1}^{n} (A - A_{\text{est}})^2 \tag{10}$$

When the error function S has been minimised between the measured characteristic matrix A and the estimated characteristic matrix A_{est} from the simplified vehicle model, the best estimates of the inertial parameters have been found. This is performed n times, which is equal to the number of pseudo-modes added to the state matrices.

For each pseudo-measurement added to the state vectors there may exist a system characteristic matrix A, from which estimates of the inertial parameters can be found using the least squares function. For example, if 100 pseudo measurements have been added to the state vectors, there exists up to 100 system characteristic matrices and, as a consequence, there will be up to 100 estimates of the mass, mass moments of inertia and centre of gravity locations. These 100 inertial parameter estimates can be averaged to find the mean estimates. In doing so, the accuracy of the estimated inertial parameters can be greatly improved by minimising the effects of the unmeasured random inputs and measurement noise.

3. Simulation results

In this section, results are presented for estimating the vehicle inertial parameters using the method shown in this paper. First, the 12DOF simulation model is presented followed by

the 3DOF estimation model used to estimate the inertial parameters. The equivalent stiffness equations for this vehicle are then found using a numerical least squares analysis. Finally, the results for four differing load conditions are presented.

3.1. *Vehicle simulation model*

The simulation model, shown in Figure 2, has twelve degrees of freedom and consists of a vehicle chassis with bounce, pitch and roll modes, four unsprung masses, an engine and up to four passengers. A front anti-roll bar is included which adds additional stiffness to the front oppositional wheel hop and sprung mass roll modes, but has minimal impact on the bounce, pitch and parallel wheel hop modes.

The sprung mass generalised coordinates left front (Z_{LF}), left rear (Z_{LR}) and right rear (Z_{RR}) are selected to represent a vehicle fitted with three accelerometers. For simplification of the simulation model, it is assumed that the chassis acts like a rigid body with no body warping, and human occupants are treated as a lumped mass. The damping and stiffness parameters used for the simulation model are detailed in Table 1. The values for seat stiffness and damping are generally in line with values taken from [55], where the stiffness and damping values are experimentally measured. The values for engine stiffness and damping are based around experimental values for a hydraulic fluid mount found in [56] plus some additional stiffness and damping from rubber mounts.

3.2. *Vehicle estimation model*

The model used to estimate the inertial properties is shown in Figure 3. The mass, mass moments of inertia and centre of gravity locations are the values that need to be identified. The only information that is known about the vehicle is the wheelbase ($a+b$), track width ($d+e$), sensor locations and equivalent stiffness parameters left front (k_{LF}), right front (k_{RF}), left rear (k_{LR}), right rear (k_{RR}) and anti-roll bar (k_{eqr}).

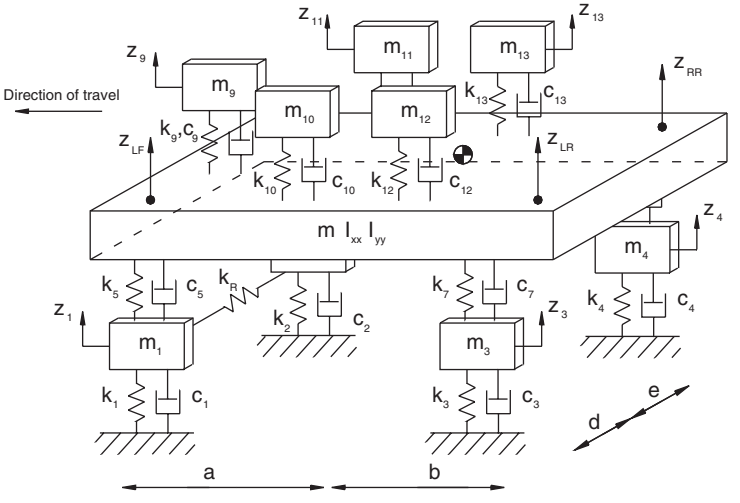

Figure 2. Twelve degrees of freedom vehicle model.

Table 1. Vehicle stiffness, damping and mass properties.

Parameter	Symbol	Value	Unit
Tire stiffness	k_1, k_2, k_3, k_4	200,000	N/m
Front suspension stiffness	k_5, k_6	45,000	N/m
Rear suspension stiffness	k_7, k_8	80,000	N/m
Anti-roll bar	k_R	50,000	N/m
Engine stiffness	k_9	550,000	N/m
Seat/body stiffness	$k_{10}, k_{11}, k_{12}, k_{13}$	75,000	N/m
Tire damping	c_1, c_2, c_3, c_4	50	N s/m
Front damping	c_5, c_6	2,800	N s/m
Rear damping	c_7, c_8	3,500	N s/m
Engine damping	c_9	6,000	N s/m
Seat/body damping	$c_{10}, c_{11}, c_{12}, c_{13}$	3,000	N s/m
Engine mass	m_9	200	kg
Front unsprung wheel mass	m_1, m_2	40	kg
Rear unsprung wheel mass	m_3, m_4	65	kg

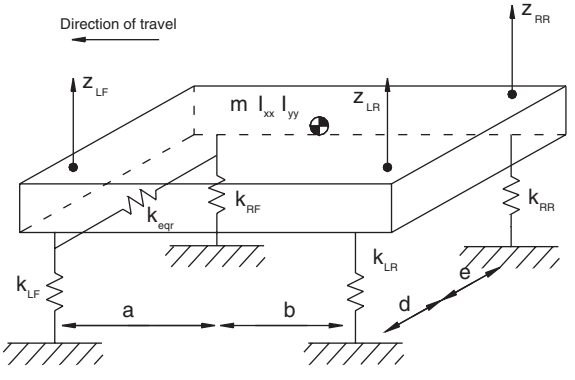

Figure 3. Three degrees of freedom estimation model.

For simplification of the estimation model, the vehicle chassis, engine and passenger masses are assumed to act as a single lumped mass, which will be referred to as the sprung mass. The sprung mass is calculated by combining the chassis, engine and occupant masses, while the equivalent pitch and roll mass moments of inertia are calculated using the parallel axis theorem.

3.3. *Equivalent stiffness equations*

For the simulation examples presented in this section, the equivalent stiffness values can be found numerically by varying the inertial properties of the 12DOF simulation model and calculating the system characteristic matrix. This can be combined with a least squares estimator and the simplified 3DOF estimation model to find the optimal values for the equivalent stiffness parameters for each loading condition. This results in a spread of equivalent stiffness parameters versus damping ratio as shown in Figure 4. A trend appears in this data which allows a mathematical relationship to be formulated, via curve-fitting, between damping ratio and equivalent stiffness.

The cluster of points to the left represents the damping ratio versus the equivalent roll bar stiffness; that to the middle is front equivalent stiffness, with the cluster of points to the right representing the rear equivalent stiffness versus damping ratio. The equivalent stiffness for

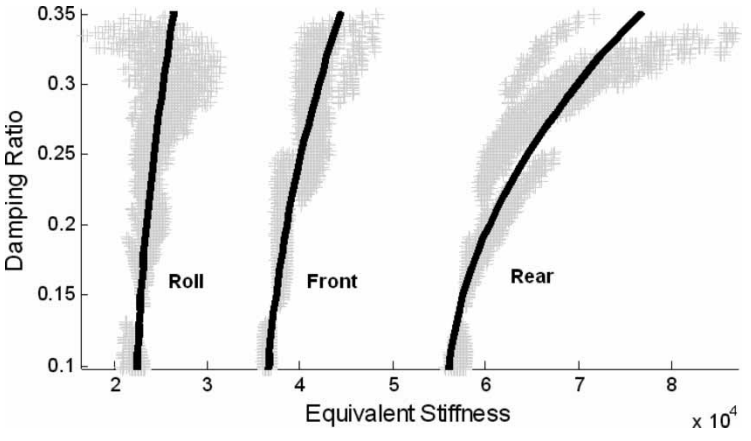

Figure 4. Equivalent stiffness versus damping ratio (damping loss factor).

this example is given by the following equations, found via a curve fitting algorithm, shown as solid black lines in Figure 4.

$$k_{\text{eqr}} = 34580\delta^2 + 190\delta + 22071 \tag{11}$$

$$k_{\text{LF}} = k_{\text{RF}} = \frac{(k_1 k_5)}{(k_1 + k_5)}(2.5044\delta^2 - 0.2638\delta + 1) \tag{12}$$

$$k_{\text{LR}} = k_{\text{RR}} = \frac{(k_3 k_7)}{(k_3 + k_7)}(4.6342\delta^2 - 0.6464\delta + 1) \tag{13}$$

where k_{eqr} is the equivalent roll stiffness, k_{LF} and k_{RF} are the front equivalent stiffness, k_{LR} and k_{RR} are the rear equivalent stiffness and δ is the average measured sprung mass damping loss factor. When the damping ratio is equal to zero, the first and second terms cancel out, and the equivalent stiffness for the front and rear suspension reduces to the standard equation for springs in series given by Equation (8). Therefore, this equation holds for the cases of damping and no damping.

For a physical vehicle, the manufacturer should have full access to simulation models of the vehicle (for example from Adams) that will allow an estimation of the frequencies and mode shapes for various load configurations, from which the system characteristic matrix could be found. An alternative is to load the vehicle with a known mass, centre of gravity and inertia. The techniques used in this paper could then be used to find the equivalent stiffness parameters. This could be completed on one vehicle during the testing phase, and then used in production cars. The interested reader is referred to [53] for a full discussion of this topic.

3.4. *Road profile*

The three-dimensional road profile is constructed using methods discussed in Cebon [49]. The spectral density of the road profile is selected to simulate a freeway road profile. The front and rear wheels drive over identical road profiles, but are delayed by a time corresponding to the wheelbase length and velocity of the vehicle, which is selected as 100 km/h for these examples.

3.5. *Simulation results*

In this section, simulation results for four differing load conditions will be presented. The first load condition simulates a vehicle with no payload and one occupant (driver) resulting in a low chassis mass, low pitch and roll inertias and a longitudinal centre of gravity with a significant forward bias. The second load condition is for the same chassis payload but with four occupants. The third load condition simulates a vehicle that has a significant payload placed at the rear of the vehicle, resulting in an increased chassis mass and inertia, and a longitudinal centre of gravity with a significant reward bias. The forth and final load condition presented has the same payload conditions as load condition 3, but with four occupants.

3.5.1. *Load condition 1*

This loading condition is typical of a vehicle carrying no cargo and a driver only. The inertial parameters used for this example are as shown in Table 2, while the stiffness and damping parameters are found in Table 1.

Using the 12DOF vehicle simulation model, simulated highway road profile and forward velocity of 100 km/h results in the following measurements at the front left, rear left and rear right chassis mounted accelerometers (Figure 5).

Table 2. Vehicle inertial parameters.

Parameter	Symbol	Value	Unit
Chassis mass	m	1300	kg
Chassis pitch mass moment of inertia	I_{yy}	2500	$\mathrm{Kg\,m^2}$
Chassis roll mass moment of inertia	I_{xx}	500	$\mathrm{Kg\,m^2}$
Chassis mass longitudinal centre of gravity	a	1.3	m
Chassis mass lateral centre of gravity	d	0.75	m
Driver	m_{10}	80	kg
Passengers	m_{11}, m_{12}, m_{13}	0	kg

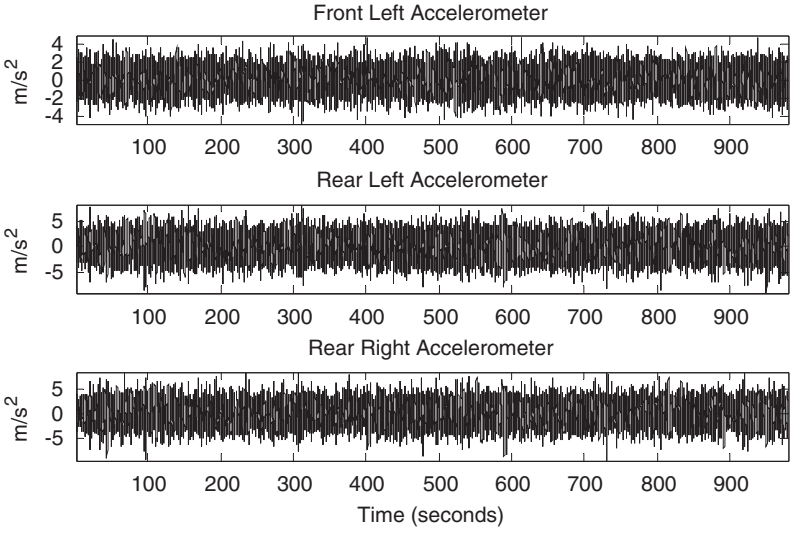

Figure 5. Sprung mass response.

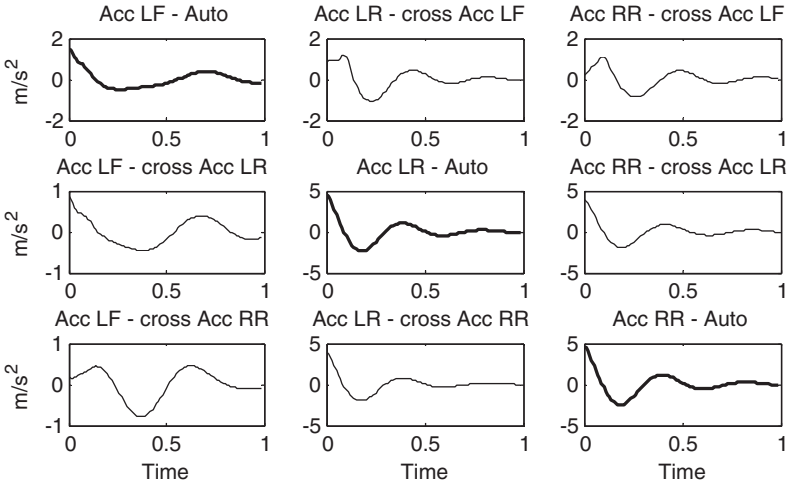

Figure 6. Extracted free-decay responses.

From these measured responses, the auto and cross correlation functions are used to extract the equivalent free-decay responses, which are shown in Figure 6.

In this figure, the auto correlations are shown diagonally and the cross correlations are shown off diagonal. The effect of the phase lag between front and rear wheel inputs can be seen in the top row of Figure 6, where some delay in the cross correlations of the left rear (LR) and right rear (RR) accelerometers can be seen. It can also be observed that the free-decay responses are not perfectly smooth, with some high frequency noise present in the results.

The state variable method is then used to estimate the system characteristic matrix based on these extracted free-decay responses. In the following examples, 100 pseudo-measurements are added to the state vectors, resulting in up to 100 estimates for the system characteristic matrices. This information is used in conjunction with the vehicle estimation model, estimated equivalent stiffness values and least squares analysis to estimate the mass, pitch and roll mass moments of inertia as well as lateral and longitudinal centre of gravity locations. These estimates can be placed in bins and represented graphically as a histogram as shown in Figure 7.

The effects of the random unmeasured excitation forces can be seen in Figure 7 as a spreading of the inertial parameter estimates. By finding the mean value of these inertial parameter estimates, this effect can be minimised, as shown in Table 3. The known mass parameter is found by simply summing the chassis, engine and occupant masses together, and the mass moments of inertia can be found by using the parallel axis theorem.

For this example, it can be seen that the estimation errors are around the 5% range.

3.5.2. *Load condition 2*

This loading condition is typical of a vehicle carrying no cargo but with four occupants. The inertial parameters used for this example are as shown in Table 4.

In an identical way to the previous example, the response of the vehicle driven over the freeway road profile with the inertial parameters noted in Table 4 is simulated. From this response, the auto- and cross-correlation functions are used to extract the equivalent free-decay responses. The state variable method is used to estimate the system characteristic matrices based on the measured free-decay responses, from which estimates of the inertial parameters can be found, as shown in Figure 8.

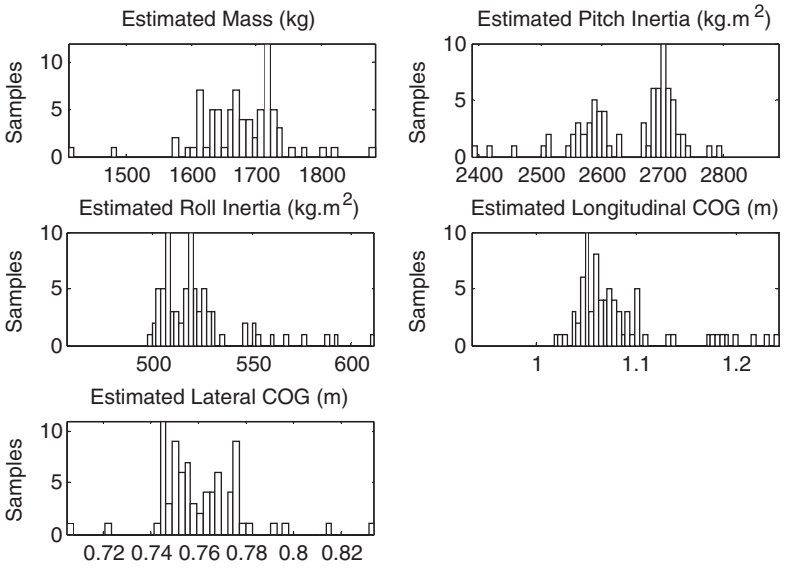

Figure 7. Estimated inertial parameters for load condition 1.

Table 3. Equivalent vehicle inertial parameters.

	Mass, m (kg)	Pitch inertia, I_{yy} (kg m^2)	Roll inertia, I_{xx} (kg m^2)	Longitudinal centre of gravity, a (m)	Lateral centre of gravity, d (m)
Known	1580.0	2752.6	515.8	1.134	0.721
Estimated	1677.7	2644.2	522.6	1.083	0.761
Mean	97.70	−108.40	6.82	−0.051	0.039
error	5.8%	−4.1%	1.3%	−4.7%	5.2%

Table 4. Vehicle inertial parameters.

Parameter	Symbol	Value	Unit
Chassis mass	M	1300	kg
Chassis pitch mass moment of inertia	I_{yy}	2500	kg m^2
Chassis roll mass moment of inertia	I_{xx}	500	kg m^2
Chassis mass longitudinal centre of gravity	a	1.3	M
Chassis mass lateral centre of gravity	d	0.75	m
Driver	m_{10}	80	kg
Passengers	m_{11}, m_{12}, m_{13}	80	kg

From these estimates, the mean values can be found and are shown in Table 5. The known mass parameter is found by simply summing the chassis, engine and occupant masses, and the mass moments of inertia can be found by using the parallel axis theorem.

3.5.3. *Load condition 3*

For this example, the vehicle is simulated to have a 500 kg cargo load placed at the rear of the vehicle, with a single vehicle driver only. This load configuration increases the chassis mass, increases the pitch and roll mass moments of inertia and shifts the longitudinal centre of gravity location reward as shown in Table 6.

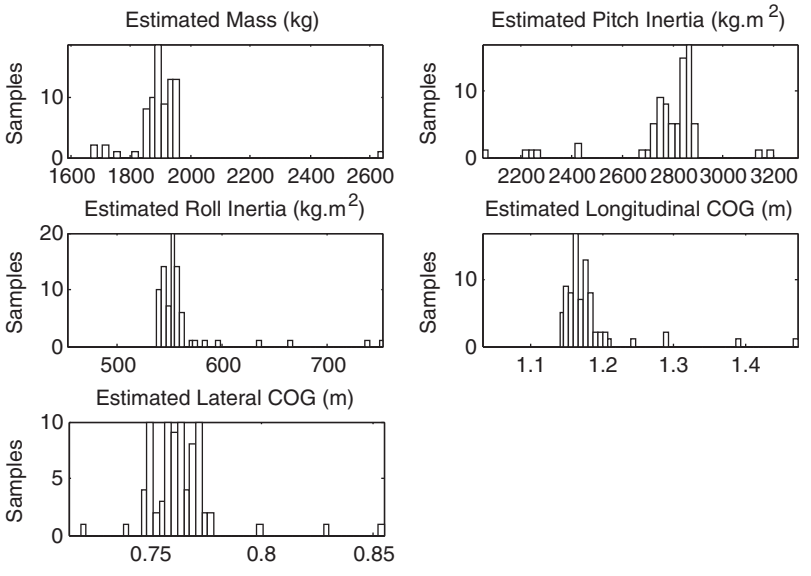

Figure 8. Estimated inertial parameters for load condition 2.

Table 5. Equivalent vehicle inertial parameters.

	Mass, m (kg)	Pitch inertia, I_{yy} (kg m^2)	Roll inertia, I_{xx} (kg m^2)	Longitudinal centre of gravity, a (m)	Lateral centre of gravity, d (m)
Known	1820.0	2863.8	552.1	1.203	0.736
Estimated	1905.6	2773.5	559.8	1.179	0.763
Mean	85.60	−90.30	7.64	−0.024	0.028
error	4.5%	−3.3%	1.4%	−2.1%	3.6%

Table 6. Vehicle inertial parameters.

Parameter	Symbol	Value	Unit
Chassis mass	m	1800	kg
Chassis pitch mass moment of inertia	I_{yy}	3500	kg m^2
Chassis roll mass moment of inertia	I_{xx}	900	kg m^2
Chassis mass longitudinal centre of gravity	a	1.8	m
Chassis mass lateral centre of gravity	d	0.75	m
Driver	m_{10}	80	kg
Passengers	m_{11}, m_{12} , m_{13}	0	kg

In an identical way to the previous example, the response of the vehicle with the inertial parameters noted in Table 6 is simulated and the inertial parameters estimated as shown in Figure 9 (see also Table 7).

3.5.4. *Load condition 4*

For this final example, the vehicle is simulated to have a 500 kg cargo placed at the rear of the vehicle in addition to four vehicle occupants, as shown in Table 8.

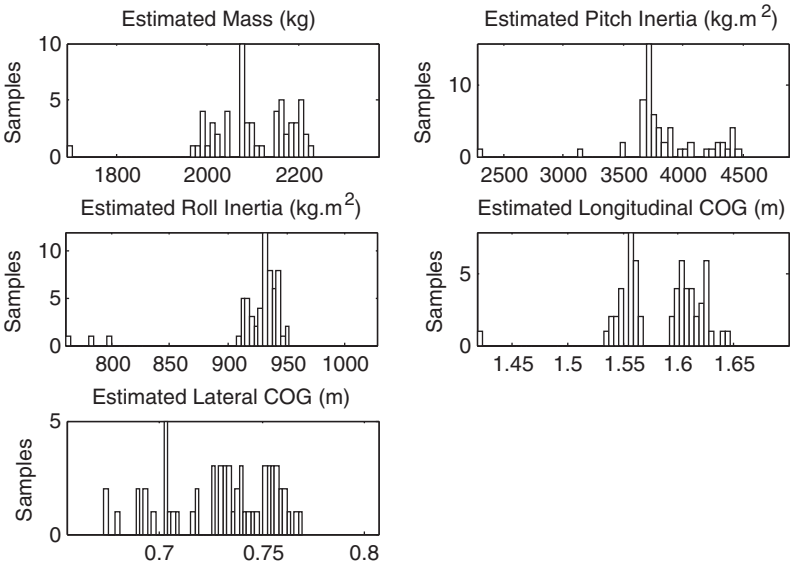

Figure 9. Estimated inertial parameters for load condition 3.

Table 7. Equivalent vehicle inertial parameters.

	Mass, m (kg)	Pitch inertia, I_{yy} (kg m^2)	Roll inertia, I_{xx} (kg m^2)	Longitudinal centre of gravity, a (m)	Lateral centre of gravity, d (m)
Known	2080.0	4051.4	916.1	1.606	0.728
Estimated	2097.9	3839.3	923.4	1.585	0.731
Mean	17.90	−212.10	7.21	−0.021	0.003
error	0.9%	−5.5%	0.8%	−1.3%	0.4%

Table 8. Vehicle inertial parameters.

Parameter	Symbol	Value	Unit
Chassis mass	M	1800	kg
Chassis pitch mass moment of inertia	I_{yy}	3500	kg m^2
Chassis roll mass moment of inertia	I_{xx}	900	kg m^2
Chassis mass longitudinal centre of gravity	A	1.8	m
Chassis mass lateral centre of gravity	D	0.75	m
Driver	m_{10}	80	kg
Passengers	m_{11}, m_{12} , m_{13}	80	kg

In an identical way to the previous example, the response of the vehicle with the inertial parameters noted in Table 8 is simulated and the inertial parameters estimated as shown in Figure 10.

From these estimates, the mean values can be found and are shown in Table 9.

3.6. *Discussion*

It has been shown by way of simulation examples that estimation of the inertial parameters is achievable, with maximum relative errors for the simulation examples provided of just over 6%. Considering the inputs to the system that are assumed unknown, it is believed that this

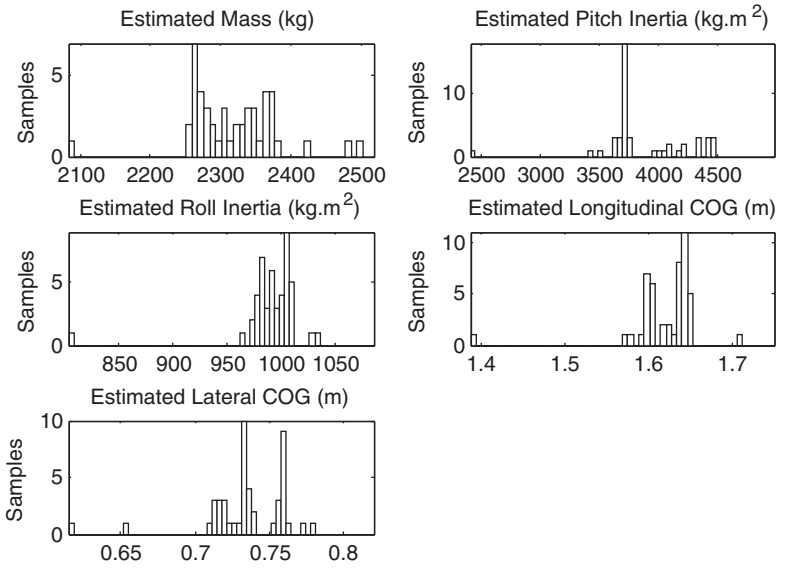

Figure 10. Estimated inertial parameters for load condition 4.

Table 9. Equivalent vehicle inertial parameters.

	Mass, m (kg)	Pitch inertia, I_{yy} (kg m^2)	Roll inertia, I_{xx} (kg m^2)	Longitudinal centre of gravity, a (m)	Lateral centre of gravity, d (m)
Known	2320.0	4104.9	952.2	1.612	0.739
Estimated	2318.0	3864.8	991.3	1.622	0.735
Mean error	−2.00	−240.10	39.06	0.010	−0.004
	−0.1%	−6.2%	3.9%	0.6%	−0.5%

result will be acceptable in most instances; in particular, this method will be useful for vehicles where the increased cost of a method that requires the input forces to be measured cannot be justified. Although the estimated vehicle inertial properties may be considered as a rough approximation of the true values, the proposed method offers a cost-effective approach for on-board estimation of key inertial properties of a vehicle with improved accuracy when compared with those existing techniques. Nevertheless, in real-world applications, the maximum relative error in estimation may be larger than 6% as there are several potential sources of errors, as discussed below.

The estimation errors are produced from several sources. The first is inaccuracies in the computed auto- and cross-correlation functions. It is assumed that these measurements are proportional to the free-decay responses which, in a strict mathematical sense, can only occur when the system is excited by pure white Gaussian noise. Therefore some estimation errors will occur due to the road profile input not having a white Gaussian noise spectrum.

A second error source is inaccuracies in the equivalent stiffness parameters. This numerically derived equation relies on an accurate measurement of the damping loss factor which may be inaccurately estimated due to errors in the extracted free-decay responses. It can also be seen in Figure 4 that these numerically derived equivalent stiffness equations are a best guess fit of the optimal values for all possible loading conditions. It is likely that the optimal equivalent stiffness parameter will not lie on the line of best fit and as a consequence this will introduce some error into the inertial parameter estimates.

Other sources of error include the delay between the front and rear inputs, which are related to the wheelbase length and forward velocity. In these simulations, the time delay between front and rear inputs is sufficiently short and so is not a concern. However, it has been observed that as the speed of the vehicle decreases, the time delay between inputs increases and does affect the estimation accuracy of the pitch mass moment of inertia; so forward velocity of the vehicle is one limitation of this method.

The estimation model assumes the measurement sensor, and principal moments of inertia are aligned along the same axis. This means the products of inertia are not measured and will result in some additional error for the estimated moments of inertia. These errors will be quantified by way of simulation and experiments in subsequent publications. On-road experiments with a real vehicle are currently underway with promising preliminary results. The results for these experimental tests will be presented in subsequent publications once a detailed analysis has been completed.

4. Conclusion

A method for the estimation of mass, centre of gravity and mass moments of inertia of a vehicle while in motion and subjected to unknown random excitation forces has been presented. An approach is also proposed for determining the equivalent suspension stiffness coefficients, when the vehicle is simplified as a 3 degrees of freedom system, based on measurement of the damping loss factors. The use of auto-correlation functions computed from measured sprung mass random responses allows the free-decay responses to be computed while the vehicle is in motion, allowing modal analysis techniques to be used. Simulation results indicate that the relative errors of the estimated vehicle inertial properties are reasonably small. Further work is currently underway to quantify estimation errors, using experimental measurements.

Acknowledgements

This work is supported by the ARC Centre of Excellence programme and a Discovery Project (DP 0773415) that are funded by the Australian Research Council.

References

[1] G. Heydinger, R. Bixel, N. Durisek, E. Yu, and D. Guenther, *Effects of loading on vehicle handling*, SAE Technical Paper Series, 980228, 1998.
[2] P. Yih, *Steer by wire – implications for vehicle handling and safety*, Ph.D. dissertation, Stanford University, 2005.
[3] M. Arndt, C. Dickerson, and S. Ardnt, *Influence of passenger and cargo load on the at limit handling of a mini van*, SAE Technical Paper Series, 1999-01-0449, 1999.
[4] R. Whitehead, W. Travis, D. Bevly, and G. Flowers, *A study of the effects of various vehicle properties on rollover propensity*, SAE Technical Paper Series, 2004-01-2094, 2004.
[5] A. Hac, *Rollover stability index including effects of suspension design*, SAE Technical Paper Series, 2002-01-0965, 2002.
[6] T. Gillespie, *Fundamentals of vehicle dynamics*, Society of Automotive Engineers, ISBN 1-56091-199-9, 1993.
[7] T. Sun, Y. Zhang, and P. Barak, *4-DOF vehicle ride model*, SAE Technical Paper Series, 2002-01-1580, 2002.
[8] J. Goncalves and J. Ambrosio, *Road vehicle modelling requirements for optimization of ride handling*, Multibody System Dynam. 13(1) (2005), pp. 3–23.
[9] J. Grieser, *Method for determining an estimate of the mass of a motor vehicle*, Patent number US6980900, 2005.
[10] A. Hac, *Effects of brake actuator error on vehicle dynamics and stability*, SAE Technical Paper Series, 2005-01-1578, 2005.
[11] H. Navarro and A. Canale, *Influences of the load centre of gravity on heavy vehicle acceleration*, Int. J. Heavy Vehicle Systems 8 (2001), pp. 17–47.

[12] B. Chen and H. Peng, *Differential braking based rollover prevention for sport utility vehicles with human-in-the-loop evaluations*, Vehicle System Dynam. 36(4–5) (2001), pp. 359–389.
[13] M. Boada, B. Boada, A. Munõz, and Díaz, *Integrated control of front-wheel steering and front braking forces on the basis of fuzzy logic*, Proc. Inst. Mech. Eng., Part D 220(3) (2006), pp. 253–267.
[14] A. Hac, D. Doman, and M. Oppenheimer, *Unified control of brake and steer-by-wire systems using optimal control allocation methods*, SAE Technical Paper Series, 2006-01-0924, 2006.
[15] S. Bickerstaffe (2006) *Bosch adds load sensing to electronic stability kit*, Automotive Engineer, May 2006, 31(5) p. 44.
[16] K. Mueller and B. Rappenau, *Method and device for ascertaining the laden state of a vehicle*, Patent number US6604025, 2003.
[17] E. Bedner, D. Fulk, and A. Hac, *Exploring the trade-off of handling stability and responsiveness with advanced control systems*, SAE Technical Paper Series, 2007-01-0812, 2007.
[18] H. Gao, J. Lam, and C. Wang, *Multi-objective control of vehicle active suspension systems via load-dependant controllers*, J. Sound Vib. 290 (2006), pp. 654–675.
[19] Z. Yong, S. Jian, W. Di, and X. Chunxin, *Automatic transmission shift point control under different driving vehicle mass*, SAE Technical Paper Series, 2002-01-1258, 2002.
[20] M. Liubakka, D. Rhode, J. Winkelman, and P. Kokotovic, *Adaptive automotive speed control*, IEEE Trans. Automat. Control 38(7) (1993), pp. 1011–1020.
[21] G. Marsden, M. McDonald, and M. Brackstone, *Towards an understanding of adaptive cruise control*, Transportation Res. C. 9(1) (2001), pp. 35–51.
[22] P. Ioannou, Z. Eckert, and C. Sieja, *Intelligent cruise control: theory and experiment*, Proceedings of the 32nd Conference on Decision and Control, 15–17 December 1993, San Antonio, TX, pp. 1885–1890.
[23] K. Yi, J. Hong, and Y. Kwon, *A vehicle control algorithm for stop-and-go cruise control*, Proc. Inst. Mech. Eng. Part D 215(10) (2001), pp. 1099–1115.
[24] F. Lattemann, K. Neiss, S. Terwen, and T. Connolly, *The predictive cruise control – a system to reduce fuel consumption of heavy duty trucks*, SAE Technical Paper Series, 2004-01-2616, 2004.
[25] G. Heydinger, R. Bixel, W. Garrot, Pyne, J. Howe, and D. Guenther, *Measured vehicle inertial parameters NHTSA's data through November 1998*, SAE Technical Paper Series, 1999-01-1336, 1999.
[26] W. Garrott, M. Monk, and J. Chrstos, *Vehicle inertial parameters – measured values and approximations*, SAE Technical Paper Series, 881767, 1998.
[27] A. Vahidi, A. Stefanopoulou, and H. Peng, *Experiments for online estimation of heavy vehicle's mass and time-varying road grade*, Proceedings of the ASME International Mechanical Engineering Congress and Exposition, Washington, DC, November 2003, pp. 4951–4956.
[28] A. Vahidi, A. Stefanopoulou, and H. Peng, *Recursive least squares with forgetting for online estimation of vehicle mass and road grade*, Vehicle Systems Dynam. 43(1) (2005), pp. 31–55.
[29] E. Ritzen, *Adaptive vehicle weight estimation*, Ph.D. Dissertation, Linköping University, 1998.
[30] H. Bae, J. Ryu, and J. Gerdes, *Road grade and vehicle parameter estimation for longitudinal control using GPS*, Proceedings of the IEEE Conference on Intelligent Transportation Systems, Oakland, CA, 25–29 August 2001, pp. 160–171.
[31] H. Bae and J. Gerdes, *Parameter estimation and command modification for longitudinal control of heavy vehicles*, 2003, Californian PATH Research Report, 2003.
[32] M. Druzhinina, A. Stefanopoulou, and L. Moklegaard, *Adaptive continuously variable compression braking control for heavy-duty vehicles*, J. Dynam. Systems Meas. Control 124(3) (2002), pp. 406–414.
[33] V. Winstead and I. Kolmanovsky, *Estimation of road grade and vehicle mass via model predictive control*, Proceedings of the IEEE Conference on Control Applications, 28–31 August 2005, pp. 1588–1593.
[34] T. Massel, E. Ding, and M. Arndt, *Estimation of vehicle loading state*, Proceedings of the International Conference on Control Applications, Taipei, Taiwan, 2–4 September 2004, pp. 1260–1265.
[35] K. Leimbach, H. Veil, and S. Hummel, *Method and system for determining a vehicle mass*, Patent number US6314383, 2001.
[36] T. Wenzel, K. Burnham, M. Blundell, and R. Williams, *Dual extended Kalman filter for vehicle state and parameter estimation*, Vehicle System Dynam. 44(2) (2006), pp. 153–171.
[37] M. Russo, R. Russo, and A. Volpe, *Car parameters identification by handling manouvres*, Vehicle System Dynam. 34(6) (2000), pp. 423–436.
[38] P. Venhovens and K. Naab, *Vehicle dynamics estimation using Kalman filters*, Vehicle System Dynam. 32 (1999), pp. 171–184.
[39] H. Pacejka and I. Besselink, *Majic tire formula model with transient properties*, Vehicle System Dynam. 27 (1997), pp. 234–249.
[40] R. Tal and S. Elad, *Method for determining weight of a vehicle while in motion*, Patent number US5973273, 1998.
[41] D. Sol and S. Watanabe, *Vehicle inertia and center of gravity estimator*, Patent number US5136513, 1992.
[42] G. Venture, P. Bodson, M. Gautier, and W. Khalil, *Identification of the dynamic parameters of a car*, SAE Technical Paper Series, 2003-01-1283, 2003.
[43] P. Bolzern, F. Cheli, G. Falciola, and F. Resta, *Estimation of the non-linear suspension tyre cornering forces from experimental road test data*, Vehicle System Dynam. 31(1) (1999), pp. 23–34.
[44] A. Best, *Vehicle ride – stages in comprehension*, Phys. Technol. 15 (1984), pp. 205–210.
[45] J. Asmussen, *Modal analysis based on the random decrement technique*, Ph.D. Dissertation, University of Aalborg, Denmark, 1997.

[46] J. Bendat and A. Piersol, *Random Data – Analysis and Measurement Procedures*, Wiley-Interscience, New York, 1971, ISBN 0-471-06470-X.
[47] A. Kareem and K. Gurley, *Damping in structures: its evaluation and treatment of uncertainty*, J. Wind Eng. Ind. Aerodyn. 59 (1996), pp. 131–157.
[48] G. James and T. Carne, *The natural excitation technique (next) for modal parameter extraction from operating structures*, Int. J. Anal. Exp. Modal Anal. 10(4) (1995), pp. 260–277.
[49] Y. Zhang, Z. Zhang, X. Xu, and H. Hua, *Modal parameter identification using response data only*, J. Sound Vib. 282 (2005), pp. 367–380.
[50] D. Cebon, *Handbook of Vehicle-Road Interaction*, Swets & Zeitlinger, ISBN 90-265-1554-5, 2000.
[51] M.R. Haddara and M. Wishahy, *An investigation of roll characteristics of two full scale ships at sea*, Ocean Eng. 29 (2002), pp. 651–666.
[52] J. He and Z. Fu, *Modal Analysis*, Butterworth-Heinemann, London, ISBN 0 7506 5079 6, 2001.
[53] N. Zhang and S. Hayama, *Identification of structural system parameters from time domain data (direct identification of mass, stiffness and damping parameters of a structure)*, JSME Ser. III 34(1) (1991), pp. 64–71.
[54] N. Zhang and S. Hayama, *Identification of structural system parameters from time domain data (identification of global modal parameters of a structural system by improved state variable method)*, JSME Series III 33(2) (1990), pp. 168–175.
[55] M. Rozyn, *Estimation of vehicle inertial parameters*, Ph.D. dissertation, University of Technology, Sydney, 2008.
[56] A. Geisberger, *Hydraulic engine mount modeling, parameter identification and experimental validation*, Master of Applied Science in Mechanical Engineering, University of Waterloo, Ontario, 2000.